Optik 126 (2015) 599–602

Contents lists available at ScienceDirect

Optik

journal homepage: www.elsevier.de/ijleo

Influence of the permeable layer number of porous silicon microcavity on reflection spectrum

Hongyan Zhang[a,*], Zhenhong Jia[b], Xiaoyi Lv[b], Rong Wu[a], Peng Li[a], Jing Wang[a]

[a] School of Physical Science and Technology, Xinjiang University, Urumqi 830046, PR China
[b] Colleges of Information Science and Engineering, Xinjiang University, Urumqi 830046, PR China

ARTICLE INFO

Article history:
Received 23 January 2014
Accepted 27 January 2015

Keywords:
Multilayer porous silicon
Permeable layer number
Reflectance spectrum
Biosensor

ABSTRACT

The influence of permeable layer number of porous silicon microcavity (PSM) on the reflectance spectrum has been carried out from both simulations and experiments. The increase of the effective refractive index of the first porous silicon (PS) layer of PSM will causes a blue shift for the reflectance spectrum. With one more layer refractive index increasing, the blue shift becomes less, and it will shift to a higher wavelength when the layer number becomes large enough. This study would be helpful for simple fabrication of highly sensitive, fast responsible biosensors based on the blue shift of reflectance spectrum, and such fabricated Au/PSM substrate of multilayer PS might have a potential to detect minor biomolecules by means of surface state effects.

1. Introduction

Porous silicon (PS) has a sponge-like structure and large internal surface-to-volume ratio which can reach several hundreds of square meters per cubic centimeter, and hence they are size-selective to contaminant species [1–3]. The large value accounts for the enhanced reactivity of PS with various adsorptive substances. The adsorption of chemical or biological molecules into the pores results in a change of optical and electrical properties of PS, such as reflectance, photoluminescence and electrical conductivity [4–6]. Therefore, PS is considered as almost an ideal optical sensor platform due to its interesting morphological and physical properties. Currently, photonic structures are widely used as transducer for sensing applications based on a change in effective refractive index due to biomolecules attachment events [7,8]. PS has been also used to fabricate one-dimensional or two-dimensional photonic structure for sensing and communication [9–11]. The most important property of the photonic structures is the photonic band structure and the photonic band gap that the geometry creates, where the light is prohibited to propagate inside the material, or it is allowed to propagate only in certain directions at certain frequencies. Various complicated PS-based configurations have emerged as optical biochemical sensors, such as Bragg mirrors, waveguides, microcavities, grating waveguides, and so on [12–14]. Nevertheless, the most widely used PS-based photonic designs are multilayer PS due to the ease of preparation by periodically altering the etching time and etching current. Among these photonic structures, porous silicon microcavities (PSM) attract great interests of many scientists in label free optical biosensor, resulting from its interesting optical properties such as high reflectivity stop band with a sharp reflectance dip in its center of reflectance spectrum, which can be used to achieve highly sensitive biosensors. It is well known that molecules adsorbed on the internal pore walls, cause an increase of the average refractive index of multilayer PSM, and hence cause a resonance peak shift toward longer wavelength (red shift). However, In general procedure for fabrication and detection of PSM biosensor, chemical agents or biomolecules are probably not enter fully into all of the PS layers of PSM, which may affect the accuracy and sensitivity of multilayer PSM.

The objective of this study is to develop PSM sensors based on porous silicon multilayer. A photonic model for a multilayer PSM is presented and the reflectance spectra are discussed from both experiments and theory when the refractive index changes for different number of surface layers of PSM.

2. Experiment procedure

2.1. Reagents and instruments

3-Aminopropyltriethoxysilane (APTES) and chloroauric acid ($HAuCl_4{\cdot}4H_2O_2$, 48–50% Au basis) were purchased from Aladdin Reagent Co. (China, www.aladdin-reagent.com). Phosphate buffer saline pH 7.4 (0.01 M PBS buffer solution) was obtained from the key

* Corresponding author. Tel.: +86 13999839908; fax: +86 09918582405.
E-mail address: zhanghongyanxj@163.com (H. Zhang).

http://dx.doi.org/10.1016/j.ijleo.2015.01.026
0030-4026/

laboratory of Xinjiang biological resources and gene engineering. All the chemicals were of analytical reagent grade.

Reflectance spectrum was measured by UV–vis scanning spectrophotometer (Hitachi, U-4100, Japan) in the wavelength ranging from 400.00 nm to 2000.00 nm. Surface image of Au/PSM substrate was obtained by a field-emission scanning electron microscope (ZEISS SUPRA 55VP, Zeiss SMT, Germany) and Cross-sectional image of Au/PSM substrate was obtained using a field-emission scanning electron microscope (Hitachi, S-4800, Japan).

2.2. Preparation of PSM

PSM was prepared by electrochemical anodization with highly doped p-type Si (boron doped, 0.01–0.02 Ω cm resistivity, 420 ± 10 μm thickness) in a mixed solution of 49% aqueous hydrofluoric acid and ethanol (1:1 by volume). The teflon etch cell that exposed 0.785 cm^2 to a Si substrate was employed and a copper electrode was immersed into the electrolyte as counter electrode. The periodic multilayer structures of PS films were fabricated by using a computer program (Labview) to alternately change current density for different etching time with a 5 s pause after each layer formation and the PSM sequence followed by $(n_L n_H)^6 n_{Lc} (n_H n_L)^6$, where n_L represents high porosity or low refractive index layer with current density of 100 mA/cm^2 for 2.3 s, n_H represents low porosity or high refractive index layer with a current density of 40 mA/cm^2 for 3.6 s, and n_{Lc} corresponds to microcavity layer formed by employing a current density of 100 mA/cm^2 for 9.2 s.

2.3. Experiments

It is well-known that when a multilayer PS is exposed to chemical or biological molecules, the effective refractive index for all PS layers of multilayer PS increases, and this increase of effective index makes overall reflectivity spectrum shift to higher wavelength, widely known as red shift. This method is used widely to detect and identify unknown chemical or biological molecules in most of PS sensing applications. But in the fabrication process of those multilayer PS biosensors, including oxidization, silanization, immobilization and detection [14,15], especially in later two cases, a small amount of solution dropped onto the prepared multilayer PS substrate can not ensure all the effective refractive index of every PS layer changes the same. Therefore in this circumstance the sensitivity and the accuracy of the sensor will be strongly influenced. Based on above consideration, we began with simulations by using the transfer matrix method to determine the change of reflectance spectra of PSM with respect to the change of effective reflective index for different permeable layers.

2.3.1. Blue shift experiments

To verify that the surface state effects of PSM structures led to a change in reflectance spectrum, the PSM substrates were immersed into 1 mM $HAuCl_4$ solution in ethanol for 4 min, 8 min, 12 min and 16 min respectively. Freshly etched PS is hydrogen terminated with Si–H hydrideds on its surface which are very responsive, reactive and unstable. Au nanoparticles (AuNPs) formed on the surface of PSM by exposing freshly PSM to alcoholic metal salt solution which can uniformly wet the H-terminated hydrophobic PS surface. The metal salt was reduced by hydrogen on the PS surface, which results in metal nanoparticle formation and HCl synthesis during this reaction [16]. The process of Au deposition in PSM can be categorized in displacement reaction according to following chemical equations [17]:

$$AuCl_4^- + 3e^- \rightarrow Au + 4Cl^-$$

$$SiH_x + 2H_2O \rightarrow SiO_2 + (4 + x)H^+ + (4 + x)e^-.$$

2.3.2. Oxidization experiments

The designed permeable layer number based on PSM will lead a change of reflectance spectrum. Since freshly etched PS is unstable due to Si–H on the surface, its storage in the air for a long period of time leads to air impurities in it, which will substantially age PS layer and degrade its surface. In order to get stable PSM, all prepared freshly PSM were soaked in H_2O_2 (30%) for 24 h at room temperature. Then the wafers were rinsed with deionized water and dried in the air. This leads to formation of Si–O and the optical characteristics of PSM become stable. In addition to stabilization, oxidation of PS also introduces hydrophilicity to the material, which is an essential requirement in biological applications.

2.3.3. Red shift experiments

10 μL, 20 μL, 30 μL and 40 μL 5% solution of APTES in water/methanol mixture (v/v = 1:1) were dropped onto the PSM substrates separately. After 2 h of incubation in 37 °C, all PSM substrates were rinsed with deionized water and dried in the air.

3. Results and discussions

As shown in Fig. 1a, the PSM is constituted of a Fabry–Perot cavity generally obtained by inserting a λ/2 layer in between two Bragg reflectors (DBRs). Each DBR consists of high and low reflective index PS layers, corresponding to alternating low and high porosity of PS, respectively. A multilayered stack is clearly observed and the microcavity layer between the two DBR PS layers can be clearly identified. The dark colored are high porosity layers and the nanocrystals are more isolated, while the white colored are low porosity layers and the nanocrystals are more densely packed. The thickness of the DBR PS layer on the silicon substrate is approximately 6.1 μm, and that of the microcavity PS layer is approximately 1.0 μm. Fig. 1b describes the structures on the PSM for the case of the Au-coated PSM. This is due to the fact that AuNPs are not embedded into the pores. Therefore the variation of Au deposition time results in the change of effective refractive index only on the surface of PSM.

Fig. 2 presents plan view SEM of AuNP deposition on the PSM for different deposition time. The sponge-like PS was obtained and the pore size varies from 10 to 20 nm. Fig. 2a shows that AuNPs deposited on the surface of the columnar PS are more homogeneous. The diameter of metal AuNPs is about 10–16 nm. When deposition time was 8 min, as in Fig. 2b, the average size of AuNPs ranges from 10 nm to 30 nm. With the increase of the deposition time, the size of individual AuNPs increases. Under the fixed salt concentration, the size dispersion increases toward larger particles with respect to the deposition time, meaning that the effective refractive index of PS increases with the increase of deposition time.

Theoretically obtainable refractive index modulation makes PSM an ideal structure for generating a strong optical confinement. Fig. 3 presents simulations from monitoring reflectance spectrum changes of PSM by using the transfer matrix method to verify the detection mechanism of the PSM as an optical sensor. Reflectance

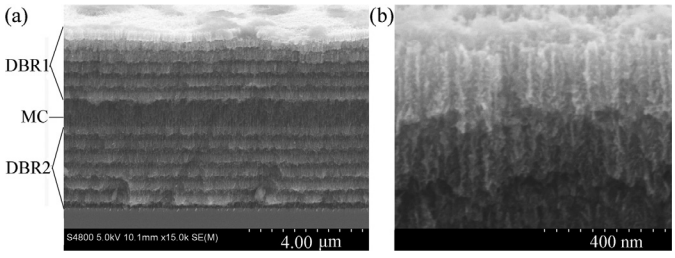

Fig. 1. (a) Cross-sectional SEM micrograph of PSM with $(n_L n_H)^6 n_{Lc} (n_H n_L)^6$ sequence. (b) High resolution cross-sectional SEM micrograph closely near surface of the PSM.